SEMARAK ILMU PUBLISHING
202103268166(003316878-P)

Journal of Advanced Research in Fluid Mechanics and Thermal Sciences

Journal homepage:
https://semarakilmu.com.my/journals/index.php/fluid_mechanics_thermal_sciences/index
ISSN: 2289-7879

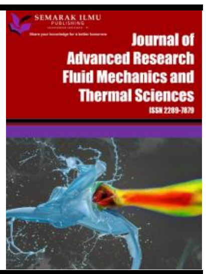

Power Optimization of The Horizontal Axis Wind Turbine Capacity of 1 MW on Various Parameters of The Airfoil, an Angle of Attack, and a Pitch Angle

Kriswanto[1,*], Muhammad Adnan Bayu Setiawan[1], Dony Hidayat Al-Janan[1], Rizqi Fitri Naryanto[1], Ahmad Roziqin[1], Hendrix Noviyanto Firmansyah[1], Rizki Setiadi[1], Febri Budi Darsono[1], Andri Setiyawan[1], Jamari[2]

[1] Department of Mechanical Engineering, Universitas Negeri Semarang, Gd E5 Kampus UNNES, Semarang, Indonesia
[2] Department of Mechanical Engineering, University of Diponegoro, Jl. Prof. Sudharto Kampus UNDIP, Semarang, Indonesia

ARTICLE INFO

Article history:
Received 25 October 2022
Received in revised form 3 February 2023
Accepted 11 February 2023
Available online 24 February 2023

Keywords:
Airfoil; angle of attack; blade element momentum; HAWT; optimization; pitch angle; wind speed

ABSTRACT

The rotor is one of the vital components of a wind turbine. In the design of the rotor, the expected result is the most optimal power. This purpose study is to optimization of the Horizontal Axis Wind Turbine power of various parameters such as airfoil, angle of attack, and pitch angle. Airfoils (NACA 4412-2412 T.E. mod, NACA 2412-4412 T.E. mod, NACA 4412-2412 L.E. mod, NACA 2412-4412 L.E. mod), angle of attack (0, 2, 4, 6), and pitch angle (0, 1, 2, 3) are the parameter variations used. The simulation method uses BEM (Blade Element Momentum), and the Taguchi for optimization is based on the L16 orthogonal array matrix. The ANOVA has to determine the contribution of each parameter to the HAWT power generated. Simulation and optimization results show that the most optimal parameter was a NACA airfoil 4412-2412 L.E mod, at 0˚ angle of attack and 0˚ pitch angle, with the resulting power reaching 1015780 Watt. The ANOVA analysis shows the airfoil parameter has the greatest contribution to the rotor power of the HAWT compared to the angle of attack and pitch angle.

1. Introduction

The Southeast Asian region has a lot of potential for using wind energy in wind turbines; one such area is Indonesia, where wind speeds can reach 4-7 m/s [1]. Therefore, based on the Beaufort scale, the wind speed is classified as low-medium [2]. Moreover, the medium wind speed classification has the potential to be utilized but has not been able to produce effective and high power. Wind speed in the range of 2 to 7 m/s is relatively suitable for small-capacity power plants, namely 10-100 kW [3], and it is necessary to develop wind energy conversion tools according to wind speed.

* *Corresponding author.*
E-mail address: kriswanto@mail.unnes.ac.id

https://doi.org/10.37934/arfmts.103.2.141156

One potential utilization of wind energy is to use a wind energy conversion tool, namely the rotor of the horizontal axis wind turbine, which is the first component of the turbine to receive wind kinetic energy to produce mechanical energy to rotate the rotor for further conversion into electrical energy [4]. Nevertheless, relatively low wind speed in Indonesia can be used because of its high efficiency [5]. Ordinarily, the design of the rotor influences the power generated, components, and parameters that are considered in designing the rotor as design a proper blade. The airfoil type, angle of attack, and pitch angle are all parameters to consider when designing HAWT's blade.

Testing the wind turbine rotor performance should be as fast and accurate as possible. One of the software that can simulate parameter values affecting wind turbines is called Qblade software. This software allows users to design airfoils and can be directly integrated into the simulation and rotor design. Besides that, there is also a method to predict wind turbine efficiency that has been designed more cost-effectively, namely BEM [6]. The BEM theory uses to analyze the rotor power of the wind turbine, optimize the rotor geometry, and analysis the force and torque acting on the blades [7].

Research related, namely the analysis of a power HAWT using a variation of NACA airfoils (0020, 0018, 0015, 0012, 5520, 5518, 5515, and 5512) found that most optimal rotor design used 55xx blades to produce a power of about 500 KW at 9m/s wind speed [8]. The study of the optimal angle of attack between the NACA 0012 blade and the NACA 2412 blade uses BEM to find that the maximum lift coefficient is when the angle of attack increases. Moreover, the NACA 2412 airfoil shows higher efficiency at a tip speed ratio of 7 and produces a maximum power compared to the NACA 0012 [9].

The study of determining the optimal angle of attack between the NACA 0012 and NACA 2412 blades to obtain the maximum lift and drag ratio using the BEM, then the result is that the NACA 2412 airfoil shows higher efficiency at a tip speed ratio of 7 and produces a maximum power output compared to the NACA 0012 airfoil [10]. The effect of setting the pitch angle with variations of displacement, namely +6°, +3°, 0°, -3°, -6° to get the power coefficient for TSR variations from 3 to 7 using BEM calculations, moreover that the pitch angle setting of 0° and +3° has the best effect on turbine efficiency [11]. Study optimization of small-scale wind turbine design on the variations of NASA airfoils, parameters angle of attack 0° to 20° obtains that lift coefficient value and lift to drag ratio best found the SD7080 airfoil [12].

The simulation and optimization of HAWT rotor power of NACA airfoils (2412 and 4412) using BEM reveals that the most optimal parameter is the NACA 4412-2412 airfoil trailing edges modified at 3° angle of attack and 8m/s wind speed [13]. Airfoil leading edge modification for wind turbine rotors by adding bumps resulted in a higher lift coefficient compared to wind turbines without additional bumps [14]. Several studies related are airfoil analysis with the addition of bumps on the wings of the aircraft to obtain better operating performance at a certain angle of attack [15-17].

The previous literature shows that even though a study on the performance analysis of HAWT has been done, the works have a specific focus on the kind of airfoil, pitch angle, and angle of attack. It is essential to understand that while using a HAWT in low wind conditions, numerous factors may have unique and concurrent effects on the airfoil variation, pitch angle, and angle of attack. In order to obtain improved parameters for the performance of the HAWT power rotor, it underlines the requirement of concurrent investigation on optimizing airfoil type, angle of attack, and pitch angles. Therefore, the goal of this study was to simulate and optimize the HAWT power from various airfoils, angles of attack, and pitch angles.

2. Methodology

This research is a simulation using BEM on Qblade Software to design and determine the rotor power. BEM is a method that can performance predict a turbine rotor [18]. The BEM is based on an estimation of the force acting on each blade segment. The blade was divided into several segments, assuming each element is independent and the fluid flow of each segment has no interaction. Following that, the force and moment of each segment will be computed. As a result, the total forces and moments are an integration of all the forces and moments of each element [19,20]. The thrust generated by the blade segment based on theory of the blade element, be determined using the equation

$$dT = B\frac{1}{2}\rho V_{total}^2 (C_l \cos\varphi + C_d \sin\varphi)\, cdr \quad (1)$$

After the thrust obtained, the torque which work on each blade segment can be calculated according to the blade element by using the equation

$$dQ = B\frac{1}{2}\rho V_{total}^2 (C_l \sin\varphi - C_d \cos\varphi)\, crdr \quad (2)$$

where *dT* is the thrust, *dQ* is the torque on the blade sections, *B* is blades number, *ρ* is the air density, V_{total} is the resultant velocity, C_l is the lift coefficient, C_d is the drag coefficient, *φ* the inflow angle, *c* is the airfoil chord, and r is the radii of the element from hub.

The force which acts on an airfoil, the chord line to the wind direction is the angle of attack (α) and the chord line to the line of rotation is the pitch angle (β) accordingly shown in Figure 1(a) and (b) [13].

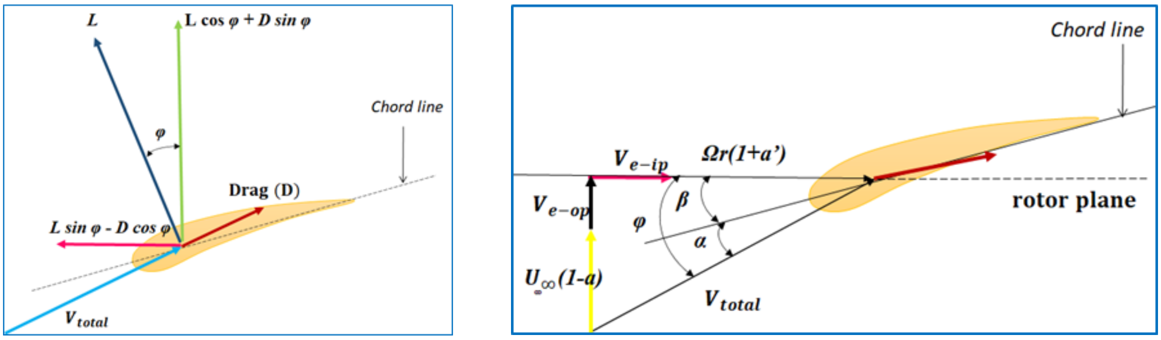

(a) (b)

Fig. 1. Local element (a) forces (b) velocities and flow angles [13]

Table 1
Parameter setup of the 1 MW HAWT Model

Specification	Value
Air density (kg/m^3)	1.225
Blades number	3
Length of blade (m)	55
Radius of hub (m)	1.25
tower height (m)	110
Swept Area (m^2)	10,023.67

The Taguchi is used to optimize the process to make a better-quality product and get more optimal results. Whereas an orthogonal array matrix, which is a matrix of the row's number and the columns arranged based on the factor's number and experiment levels, was used in designing more efficient experiments and analyzing data from simulations [21]. The main goal of Taguchi is to produce a product resistant to interference so that an optimal solution [22,23].

Ordinarily, the analysis results from the Taguchi method will display the means, signal-to-noise ratio, and standard deviations [24]. Moreover, seeing the number of variables to be taken, this model is very suitable because it provides a combination of two groups or more different variables. Taguchi has the advantage of determining the minimum number of experiments with the most effective results possible. The S/N ratio determines the factors that affect the results of power variance. It's used to study the noise factor for the results variation of parameters because it is considered stronger, simpler, and can be applied efficiently for quality improvement and control. The characteristic of the use's S/N ratio is the bigger, the better. The S/N ratio calculates the following equation

$$S/N_L = -10\ log\left(\frac{1}{n}\sum_{i=1}^{n}\frac{1}{y^2}\right) \tag{3}$$

where *y* is the value of data, and *n* is the number of samples.

This study uses 3 independent variables, each variable has 4 levels of variation, so an orthogonal array is needed to determine the minimum number of experiments to be carried out. DOF calculation conducted to find out the fewest experiments that must be done, that is

$$\begin{aligned} Total\ dof &= \text{(number of factor) x (number of level)} \\ &= 3 \text{ x } (4\text{-}1) = 9 \end{aligned} \tag{4}$$

So, it found as many as nine attempts at least. The orthogonal array matrix that will use has a level 4 standard. Nevertheless, based on the three standard OA matrices whose available values are L16, the orthogonal array matrix used is $L_{16}(4^3)$. This study also uses two-way ANOVA to analyze the effect of each parameter on the generating rotor power [25]. The output of ANOVA analysis includes the degrees of freedom for each factor, the total degrees of freedom, the degrees of freedom of error, the final percentage, the mean squared, and the F-ratio. The conditions that must be fulfilled in the ANOVA are the independence of observation, the normal of the data studied distributed, and the variance of the group must be homogeneous. The data normality test in this study used the Kolmogorov-Smirnov.

$$F\ (Xi) = f(X \geq Xi) \tag{5}$$

$$F\ (Zi) = f(\leq Zi) \tag{6}$$

$$Zi = \frac{Xi - \bar{X}}{s} \tag{7}$$

$$Di = |F(Zi)F(Xi)| \tag{8}$$

where $\bar{\bar{X}}$ is the mean of sample, $F\ (Xi)$ is the cumulative probability of the value of (Xi), $f(Xi)$ is the probability of the value (Xi), Zi is the standardized sample normal value from transformation result

(Xi), $F(Zi)$ is the cumulative probability from the value of (Zi), and Di is the result of Kolmogorov Smirnov normality.

In a study, the use of data needs to be known whether it comes from a sample or population that is uniform/homogeneous. If there are at least groups with the same data variance in a data, the data is considered uniform. Accordingly, the Barlett equation is used to determine the homogeneity of the data in this study.

$$S^2 = 1 + \frac{n\sum_{n=}^{n} x^2 - (\sum_{n=i}^{n} x^2)^2}{n(n-1)} \quad (9)$$

$$S^2 j = \frac{\sum \ db.S^2}{\sum \ db} \quad (10)$$

$$B = (\sum \quad db)\,(\log S^2\, j) \quad (11)$$

where S^2 is the square variance, *i* is the data at-i, *x* is the data value, n is the data of the number, db is the degree of freedom, and *B* is the Barlett result.

Confirmation test to determine whether the parameter settings recommended by Taguchi optimization can produce good data or vice versa. Confirmation test results can be estimated by predictive value and confidence interval using the equation

$$\mathrm{N} = \eta + \sum_{i=1}^{p} (\eta opt - \eta) \quad (12)$$

$$\eta = 1/\eta t + \sum_{i=1}^{\eta t} \eta i \quad (13)$$

where η is the mean of replication data, p is the optimal factors and levels affecting quality characteristics, ηi is the replication data at-i, ηt is the number of tests, and ηopt is the mean for optimal factors and levels.

$$Cl = \sqrt{F_{a,1,Dfe}.Ve\,.(\frac{1}{neff} + \frac{1}{r})} \quad (14)$$

$$neff = \frac{n}{1+Vt} \quad (15)$$

where Ve is the average square of the error in the ANOVA table, $F_{a,1,Dfe}$ is the F ratio at significance level a% (*F*0.5), Dfe is the degree of freedom *error* on ANOVA table, $neff$ is the total effective value, n is the number of tests, and *r* is the confirmation test number.

The study is to find the influence of variations parameters against rotor power using the Qblade software. The optimization settings of the three parameters of the HAWT rotor used are as Table 2.

Table 2
Variation of Rotor Power Optimization Parameters

Parameters	Factor	Levels			
		1	2	3	4
Pitch Angel	A	0°	1°	2°	3°
Angel of Attack	B	0°	2°	4°	6°
NACA Airfoil Type	C	4412-2412 T.E Mod	2412-4412 T.E Mod	4412-2412 L.E Mod	2412-4412 L.E Mod

Taguchi optimization with orthogonal array L_{16} is used in determining simulation parameter settings. The design of the OA matrix was adjusted to the number of factors and levels, as shown in Table 3. The L_{16} orthogonal array matrix is used in input setting parameters at Qblade software to obtain HAWT rotor output power data.

Table 3
Matriks Ortogonal Array L_{16} (4^3)

No	FACTOR A	B	C
1	4412-2412 T.E Mod	0	0
2	4412-2412 T.E Mod	2	1
3	4412-2412 T.E Mod	4	2
4	4412-2412 T.E Mod	6	3
5	2412-4412 T.E Mod	0	1
6	2412-4412 T.E Mod	2	0
7	2412-4412 T.E Mod	4	3
8	2412-4412 T.E Mod	6	2
9	4412-2412 L.E Mod	0	2
10	4412-2412 L.E Mod	2	3
11	4412-2412 L.E Mod	4	0
12	4412-2412 L.E Mod	6	1
13	2412-4412 L.E Mod	0	3
14	2412-4412 L.E Mod	2	2
15	2412-4412 L.E Mod	4	1
16	2412-4412 L.E Mod	6	0

This study uses four types of an airfoil, namely two modified NACA airfoils on the leading edge and two modified NACA airfoils on the trailing edge. All the airfoils are shown and described in Figures 2 to 5. The NACA 2412 L.E. Mod Airfoil (Figure 2) replaces the six points of coordinates on the leading edge of the NACA 2412 airfoil with six points of coordinates on the leading edge of the NACA 1410 airfoil to achieve a higher lift coefficient than the NACA 2412 standard airfoil. The NACA 2412 T.E. Mod Airfoil shown in Figure 3 was modified at six points of the trailing edge coordinates of the NACA 2412 airfoil to get a higher lift coefficient than the 2412 NACA standard airfoil [9].

The NACA 4412 L.E. Mod Airfoil (Figure 4) replaces the 11 points of coordinates on the leading edge of the NACA 4412 airfoil with 11 points of coordinates on the leading edge of the NACA 2410 airfoil to achieve a higher lift coefficient than the 4412 NACA standard airfoil.

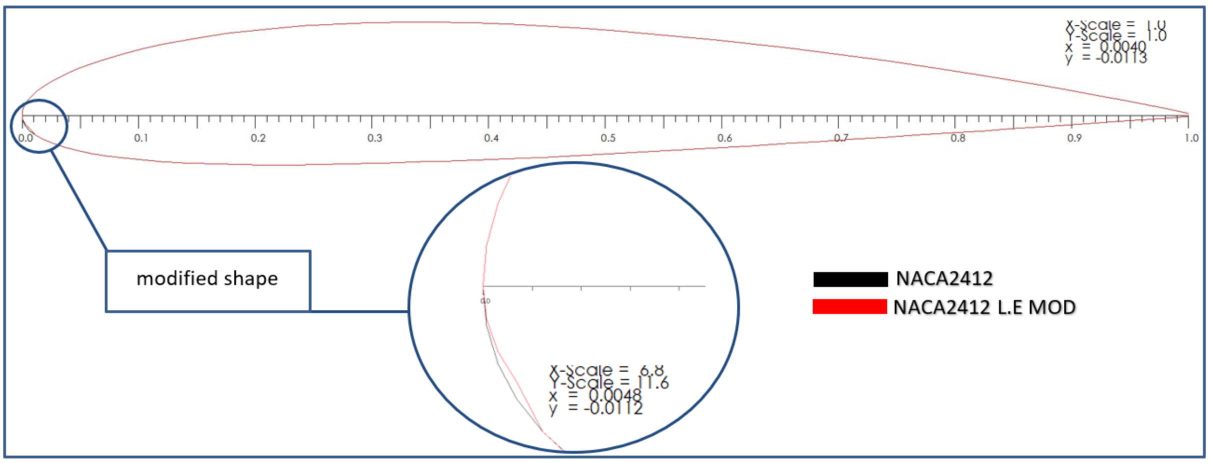

Fig. 2. Geometry of NACA 2412 L.E Mod Airfoil

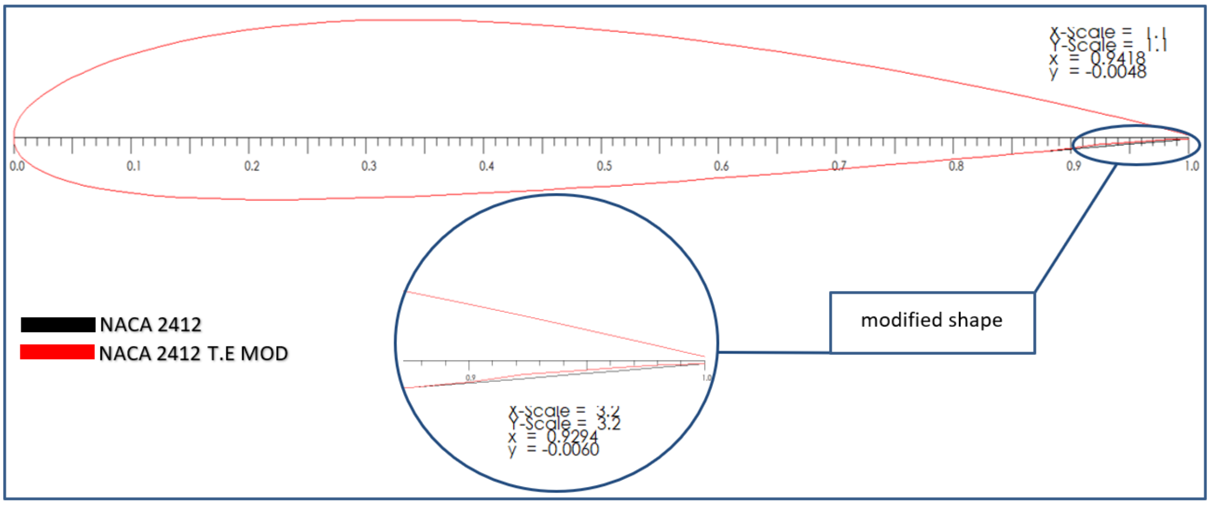

Fig. 3. Geometry of NACA 2412 T.E Mod Airfoil

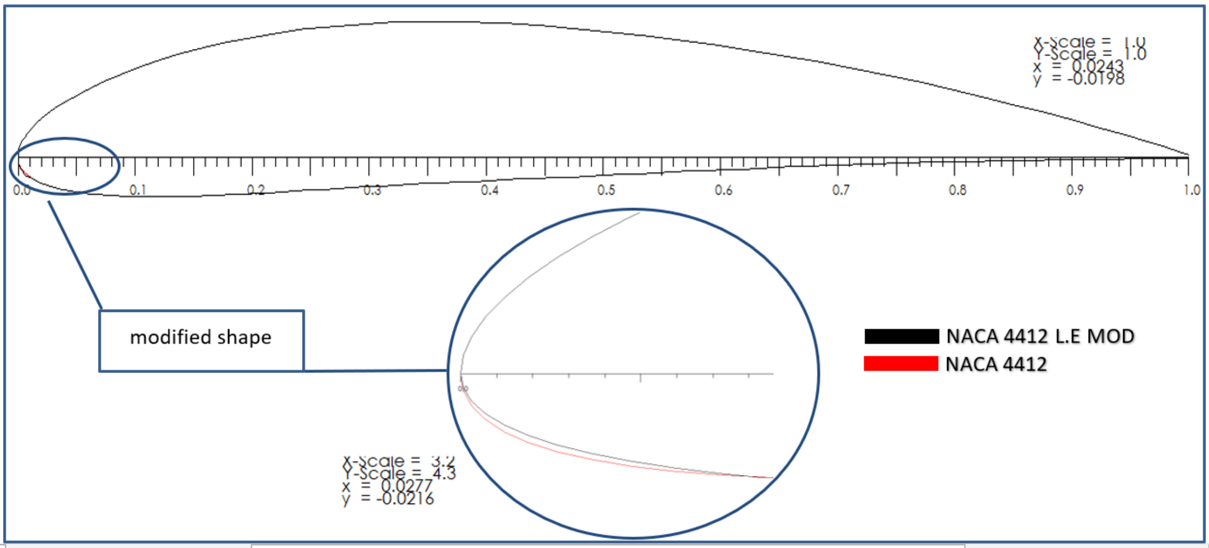

Fig. 4. Geometry of NACA 4412 L.E Mod airfoil

The NACA 4412 T.E. Mod airfoil [9] shown in Figure 5 was modified by six points of the trailing edge coordinates of the NACA 2412, so it could get a higher lift coefficient than the 4412 NACA standard airfoil.

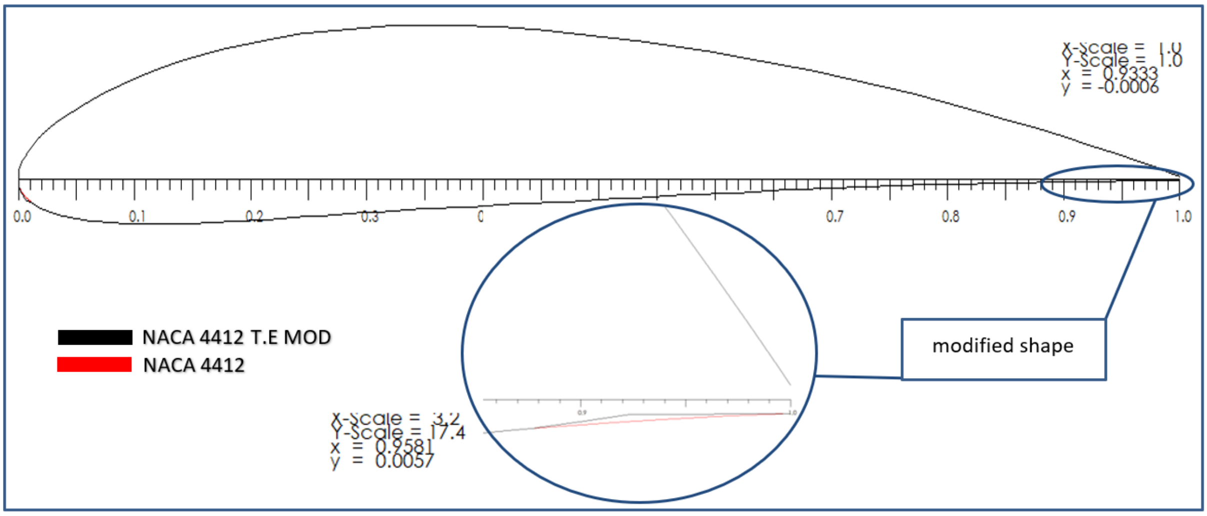

Fig. 5. Geometry of NACA 4412 T.E Mod airfoil

The HAWT blade design was conducted by inputting the airfoil in each segment. Each rotor has three blades and a 54-m radius, and the designed chord of each segment is according to the Kriswanto model [9]. Furthermore, input the angle of attack using the optimization menu on Qblade software for the optimal rotor blade design in Figure 6-9.

The blade design in Figure 6 uses circular airfoils in the first and second segments [9], then 4412 T.E. Mod airfoils in segments 3–9, and NACA 2412 T.E. Mod airfoils in segments 10–11.

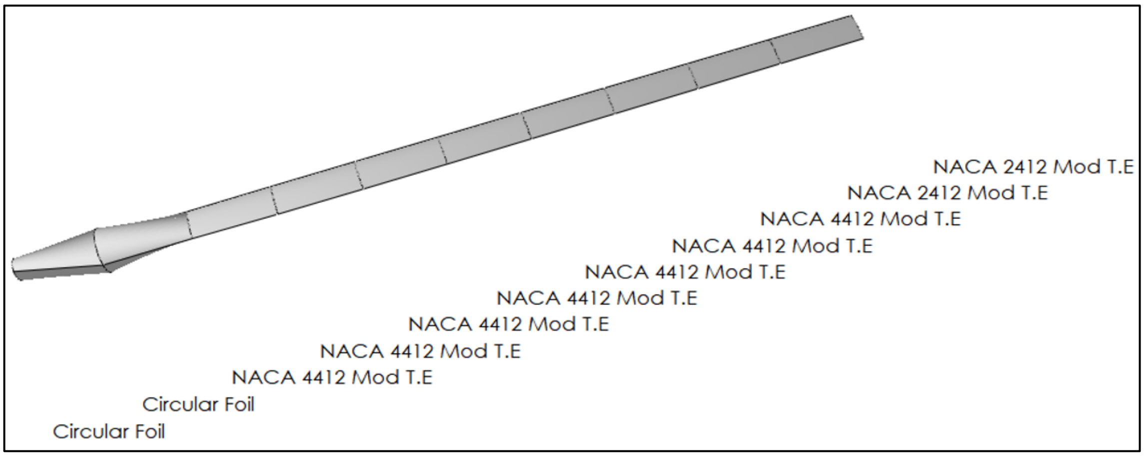

Fig. 6. Blade Design using NACA 4412-2412 T.E Mod Airfoil

The design in Figure 7 uses circular airfoils in the first and second segments following Figure 6, then NACA 2412 T.E Mod airfoils in segments 3 to 9 and NACA 4412 T.E Mod airfoils in segments 10 to 11.

The blade design in Figure 8 uses circular airfoils in the first and second segments, then NACA 4412 L.E. Mod airfoils on segments 3 to 9 and NACA 2412 L.E. Mod airfoils on segments 10 to 11.

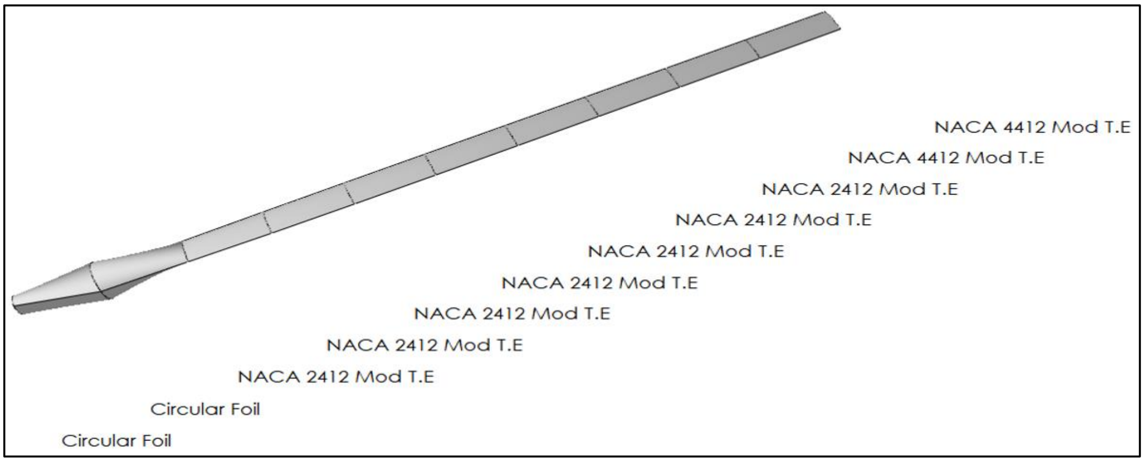

Fig. 7. Blade Design using NACA 2412-4412 T.E Mod airfoil

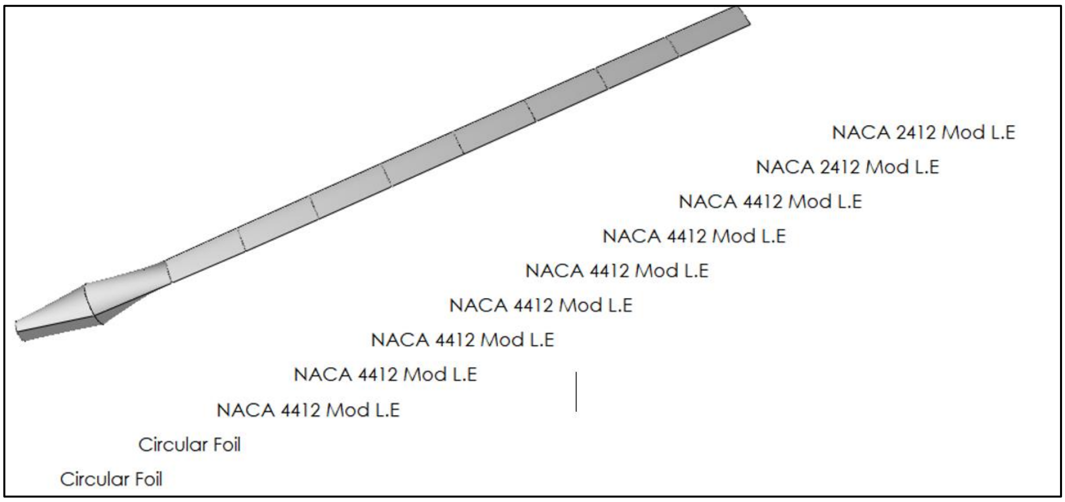

Fig. 8. Blade design using NACA 4412-2412 L.E Mod airfoil

Whereas in blade design Figure 9 NACA 2412 L.E Mod airfoils on segments 3 to 9 and NACA 4412 L.E Mod airfoils on segments 10 to 11.

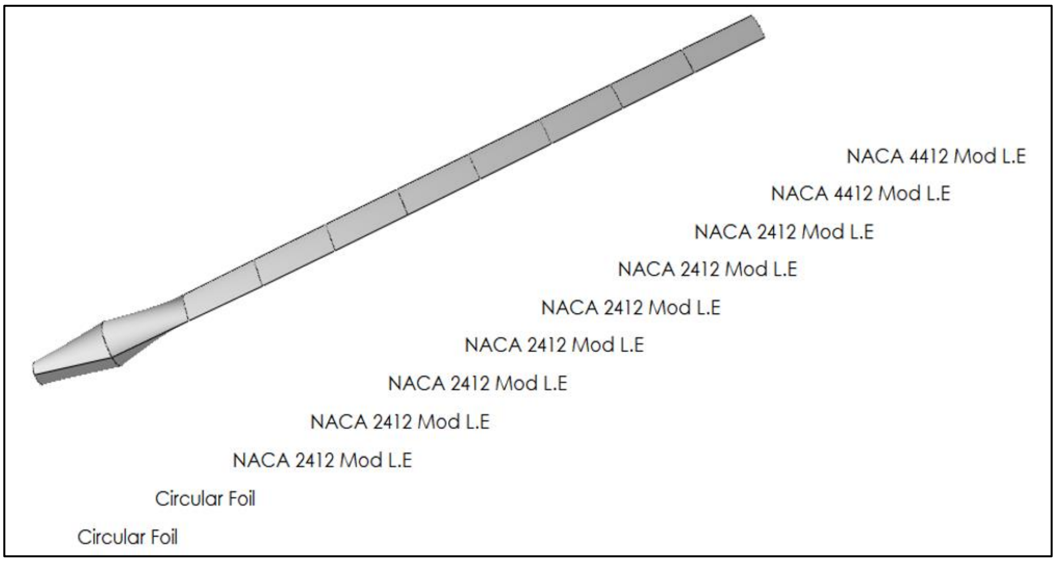

Fig. 9. Blade design using NACA 2412-4412 L.E Mod airfoil

3. Results and Discussions

This study conducted a validation test to confirm the results validity level with previous studies that used the CFD. The analysis of the rotor using the CFD with the parameters shown in Table 4 shows that, with these parameters, the CFD simulation in research [26] produces a power of 927.78 Watt.

Table 4
CFD simulation data parameter [26]

Blade Degree (°)	*Airfoil*	v (m/s)	Blade Length (m)	Density (kg/m^3)	Power (Watt)
0	0018	31.94	2.6	1.225	927.78

The rotor power simulation using the BEM compared with the CFD (Figure 12) with parameter Table 4. Accordingly, based on the BEM simulation results, the graph shows the power generated is 952 watts (Table 5).

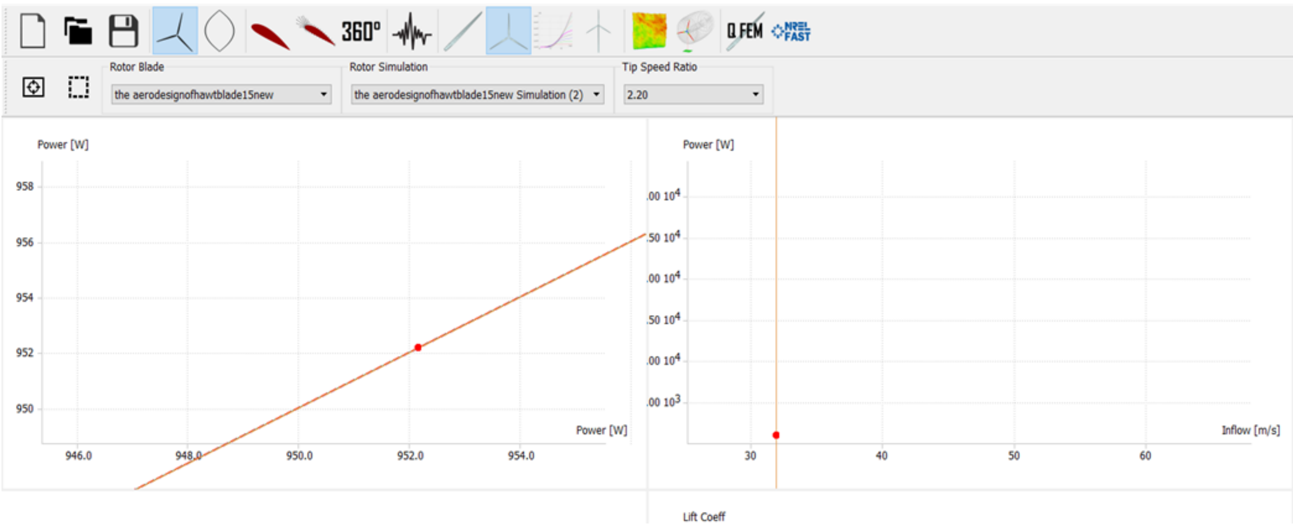

Fig. 10. Power Rotor HAWT with BEM Simulation on Qblade Software

Table 5
Comparison of Power Results Using the BEM vs CFD Metode

Simulation Method	Blade Degree (°)	*Airfoil*	v (m/s)	Blade Length (m)	TSR	Density (kg/m^3)	Power (Watt)
CFD	0	0018	31.94	2.6	-	1.225	927.78
BEM	0	0018	31.94	2.6	2.2	1.225	952

% *Error*:

$$\frac{(X2 - X1)}{X1} = \frac{(952 - 927.78)}{927.78} x\ 100 = 2.7\%$$

The results of the aerodynamic simulation between the CFD from research [27] and the BEM values are not too far apart; the percentage error result is 2.7%. Accordingly, the BEM aerodynamic simulation on the HAWT rotor follows the desired conditions. Validation was also obtained by looking at research [27] to compare the CFD and the BEM using the following rotor parameters (Table 6). Validation is performed between the two models, namely CFD and BEM, to ensure that the turbine performance values are reasonable [28]. The computational domain mesh has a significant impact on the accuracy of CFD simulation [29]. Furthermore, this method is a model for analyzing wind turbine performance based on mechanical, geometric, and feature factors [30]. The main objective of the BEM model is that it is less costly and requires less time to compute than the CFD model [31-36].

Table 6
Research Parameter Data Comparison of CFD and BEM

Radius (m)	Wind Speed (m/s)	Number of Blade	Airfoil type
1	12	3	NACA 4412

The results shown in Figure 11 shows that the difference in the coefficient of maximum power produced by the turbine using the CFD is 0.45, while BEM is 0.48, not too far away with a percent error of 6.67%, where the BEM method does not use the calculation of turbulent effects that cause the power coefficient of the result. Nevertheless, BEM simulation > power coefficient from CFD simulation [27], so the BEM aerodynamic simulation on the turbine rotor is quite close to the desired conditions.

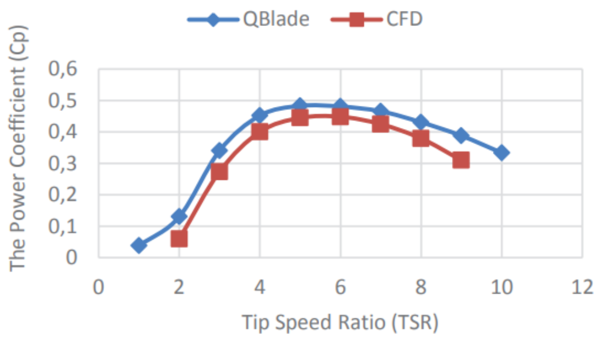

Fig. 11. Comparison of power coefficient results using Qblade BEM vs CFD [27]

$$\frac{(X2 - X1)}{X1} = \frac{(0.48 - 0.45)}{0.48} x\ 100 = 6.67\%$$

The simulation was carried out by inputting parameters in the Qblade software according to Taguchi's level, referring to the factor arrangement in Table 7. Furthermore, the results of the rotor power show that there are parameter settings capable of producing power above 1 MW.

The ANOVA was analyzed to determine the effect, contribution value, and significance level of the parameters, namely the type of airfoil, angle of attack, and pitch angle, on the HAWT rotor power. The ANOVA test on the rotor power simulation shows the airfoil type has a significant effect where the P-value is less than 0.05. As shown in Table 8, the parameters of the angle of attack and pitch angle do not have a significant effect, whereas the P-value is above 0.05. Signal-to-noise ratio (SNR) graphs aid in the interpretation of a model's behavior. However, Analysis of Variance can provide a more comprehensive understanding of the specific effects of factors [37].

Based on Table 8, the airfoil factor has a P-value less than 0.05, the angle of attack has a P-value of 0.079, and the pitch angle has a P-value of 0.461, which means that the airfoil type has a significant effect on the HAWT power compared to the angle of attack and pitch angle. The airfoil factor has the highest contribution value, i.e., 42.34%, followed by the angle of attack factor with a contribution percentage value of 32.16%, and the last is the pitch angle factor with a percentage value of 17.09%. The analysis of the average response value and signal-to-noise ratio to determine factors and set the optimal level. Table 9 shows the results of the S/N ratio for each factor level setting. Figure 10 shows a graph of the factors-levels that affect the HAWT rotor power output.

Table 7
Rotor Power Simulation Result Data

No	Factor			Power Rotor (Watt)
	Airfoil Type	Angel of Attack (°)	Pitch Angel (°)	
1	4412-2412 T.E Mod	0	0	1013803
2	4412-2412 T.E Mod	2	1	995530
3	4412-2412 T.E Mod	4	2	957850
4	4412-2412 T.E Mod	6	3	838845
5	2412-4412 T.E Mod	0	1	888720
6	2412-4412 T.E Mod	2	0	905600
7	2412-4412 T.E Mod	4	3	907220
8	2412-4412 T.E Mod	6	2	884855
9	4412-2412 L.E Mod	0	2	1006630
10	4412-2412 L.E Mod	2	3	975030
11	4412-2412 L.E Mod	4	0	976680
12	4412-2412 L.E Mod	6	1	930290
13	2412-4412 L.E Mod	0	3	907830
14	2412-4412 L.E Mod	2	2	916300
15	2412-4412 L.E Mod	4	1	903520
16	2412-4412 L.E Mod	6	0	877710

Table 8
ANOVA data result

Source	DF	Seq SS	Contribution	Adj SS	Adj MS	F-Value	P-Value
Airfoil Type	3	16704809417	42.34%	16704809417	5568269806	4.95	0.046
Angle of Attack	3	12685333787	32.16%	12685333787	4228444596	3.76	0.079
Pitch Angel	3	3316094414	8.41%	3316094414	1105364805	0.98	0.461
Error	6	6743167731	17.09%	6743167731	1123861288		
Total	15	39449405348	100.00%				

According to Table 9 and Figure 12, the optimal combination of parameter settings for HAWT rotor design is airfoil level 3, namely NACA 4412 L.E Mod-2414 L.E Mod airfoil, setting the angle of attack at level 1 (0°), and setting the pitch angle at level 1 (0°). The difference between the coefficient lifts of the NACA 4412 airfoil modification and the standard presented in Figure 13, then the angle of attack setting at level 1 (0°) and the pitch angle setting at level 1 (0°).

Table 9
Signal to noise response of rotor power

Level	Airfoil Type	Angel of Attack	Pitch Angle
1	119.54	119.6	119.48
2	119.05	119.5	119.36
3	119.75	119.4	119.47
4	119.10	118.9	119.14
Delta	0.7	0.7	0.34
Rank	1	2	3

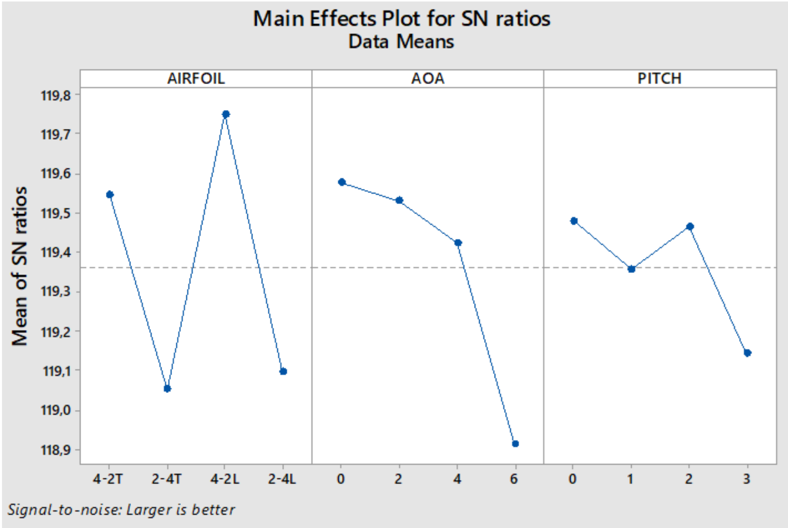

Fig 12. Signal to noise ratio graph of wind turbine power rotor

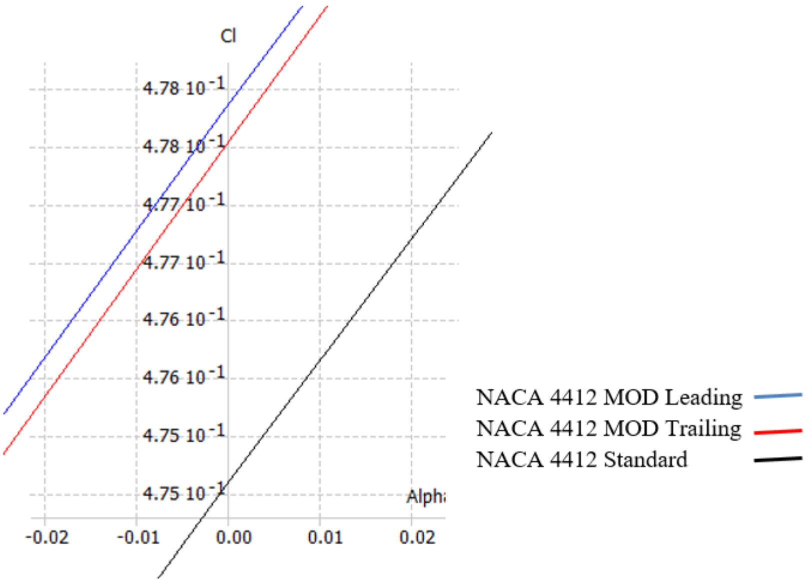

Fig. 13. Coefficient lift of NACA 4412 variation

Optimal parameter settings can give good results, and a confirmation test is carried out to strengthen the results. Before conducting a confirmation test, it is necessary to calculate the predicted value and tolerance of the power generated. Furthermore, a simulation should be carried out with the Taguchi recommendation parameters; if the confirmation test results show a value still within the interval range, the Taguchi experimental design is declared a success. The results of the predicted rotor power in the optimal parameter setting conditions (Table 9) with the optimal value of 1009050.375 Watt and interval at range ±69213.139, then a confirmation test was carried out using Taguchi recommendation parameter setting with the aim of whether the predicted value was under the confirmation result.

Accordingly, the results of the confirmation test in Table 10 show results of 1.015.780 Watt, where the confirmation test results are still within the range of the predicted value interval of 69213.139 Watt. Moreover, the value of the confirmation test was according to the design capacity of more than 1 MW.

Table 9
Prediction Value and Interval of Rotor Power

Prediction (Watt)	Interval
1009050.375	±69213.139

Table 10
Confirmation Test Result

NO	Parameter			Power (Watt)
	Airfoil type	Angle of attack (°)	Pitch angle (°)	
1	4412-2412 L.E Mod	0	0	1.015.780

4. Conclusions

HAWT power was obtained by optimizing the airfoil type parameters and the angle of attack and pitch angle on the HAWT rotor using Qblade software. The optimization method used was Taguchi orthogonal array L_{16}, and analysis of the significant parameters uses ANOVA. Based on the description, the conclusions obtained are

i. The airfoil type has the most significant effect on the HAWT power, wherein the highest contribution value of 42.34%. Nevertheless, the angle of attack and pitch angle in Qblade software does not have a significant effect on the rotor power generated by the HAWT, the attack angle setting factor has a contribution percentage value of 32.16%, and the pitch angle factor has the smallest percentage value, that is 17.09%.
ii. The most optimal HAWT rotor power obtained on the parameter's airfoil type 4412-2412 L.E Mod, angle of attack 0° and pitch angle 0°, with these settings in the Qblade software capable of producing a rotor power of 1.016 MW.

Acknowledgement
This research was not funded by any grant.

References
[1] Soeripno, M. S., and Nila Murti. "Wind hybrid power generation marketing development initiatives (WHyPGen)." *Respects Magazine* 3 (2013): 22-25.
[2] Water, Force Land. "The beaufort wind scale." (2005).
[3] Purwanto, Widodo Wahyu, Y. S. Nugroho, R. Dalimi, A. H. Soepardjo, A. Wahid, D. Supramono, D. Herminna, and T. A. Adilina. "Indonesia energy outlook and statistics." *Pengkajian Energi Universitas Indonesia, Jakarta* (2006).
[4] Islam, Md Robiul, Labid Bin Bashar, and Nazmus Sowad Rafi. "Design and simulation of a small wind turbine blade with qblade and validation with MATLAB." In *2019 4th International Conference on Electrical Information and Communication Technology (EICT)*, pp. 1-6. IEEE, 2019. https://doi.org/10.1109/EICT48899.2019.9068762
[5] Johari, M. Khudri, Muhd Jalil, and Mohammad Faizal Mohd Shariff. "Comparison of horizontal axis wind turbine (HAWT) and vertical axis wind turbine (VAWT)." *International Journal of Engineering and Technology* 7, no. 4.13 (2018): 74-80. https://doi.org/10.14419/ijet.v7i4.13.21333
[6] Marten, David, and J. Wendler. "QBlade short manual." (2018).
[7] Rezaeiha, Abdolrahim, Ricardo Pereira, and Marios Kotsonis. "Fluctuations of angle of attack and lift coefficient and the resultant fatigue loads for a large horizontal axis wind turbine." *Renewable Energy* 114 (2017): 904-916. https://doi.org/10.1016/j.renene.2017.07.101
[8] Mujahid, Muhammad, Abdur Rafai, Muhammad Imran, Mustansar Hayat Saggu, and Noor Rahman. "Design optimization and analysis of rotor blade for horizontal-axis wind turbine using Q-blade software." *Pakistan Journal of Scientific & Industrial Research Series A: Physical Sciences* 64, no. 1 (2021): 65-75. https://doi.org/10.52763/PJSIR.PHYS.SCI.64.1.2021.65.75

[9] Muhsen, Hani, Wael Al-Kouz, and Waqar Khan. "Small wind turbine blade design and optimization." *Symmetry* 12, no. 1 (2019): 18. https://doi.org/10.3390/sym12010018
[10] Oukassou, Karim, Sanaa El Mouhsine, Abdellah El Hajjaji, and Bousselham Kharbouch. "Comparison of the power, lift and drag coefficients of wind turbine blade from aerodynamics characteristics of Naca0012 and Naca2412." *Procedia Manufacturing* 32 (2019): 983-990. https://doi.org/10.1016/j.promfg.2019.02.312
[11] Rocha, PA Costa, JW Carneiro de Araujo, RJ Pontes Lima, ME Vieira da Silva, D. Albiero, C. F. de Andrade, and F. O. M. Carneiro. "The effects of blade pitch angle on the performance of small-scale wind turbine in urban environments." *Energy* 148 (2018): 169-178. https://doi.org/10.1016/j.energy.2018.01.096
[12] Suresh, A., and S. Rajakumar. "Design of small horizontal axis wind turbine for low wind speed rural applications." *Materials Today: Proceedings* 23 (2020): 16-22. https://doi.org/10.1016/j.matpr.2019.06.008
[13] Romadlon, Fajar, Dony Hidayat Al-Janan, Widya Aryadi, Rizqi Fitri Naryanto, Samsudin Anis, and Imam Sukoco. "Rotor Power Optimization of Horizontal Axis Wind Turbine from Variations in Airfoil Shape, Angle of Attack, and Wind Speed." *Journal of Advanced Research in Fluid Mechanics and Thermal Sciences* 94, no. 1 (2022): 138-151. https://doi.org/10.37934/arfmts.94.1.138151
[14] Kunya, Bashir Isyaku, Clement Olaloye Folayan, Gyang Yakubu Pam, Fatai Olukayode Anafi, and Nura Mu'az Muhammad. "Performance study of Whale-Inspired Wind Turbine Blade at Low Wind Speed Using Numerical Method." *CFD Letters* 11, no. 7 (2019): 11-25.
[15] Hakim, Muhammad Syahmi Abdul, Mastura Ab Wahid, Norazila Othman, Shabudin Mat, Shuhaimi Mansor, Md Nizam Dahalan, and Wan Khairuddin Wan Ali. "The effects of Reynolds number on flow separation of Naca Aerofoil." *Journal of Advanced Research in Fluid Mechanics and Thermal Sciences* 47, no. 1 (2018): 56-68.
[16] Ali, Jaffar Syed Mohamed, and M. Mubin Saleh. "Experimental and numerical study on the aerodynamics and stability characteristics
[17] Tajuddin, Nurulhuda, Shabudin Mat, Mazuriah Said, and Shumaimi Mansor. "Flow characteristic of blunt-edged delta wing at high angle of attack." *Journal of Advanced Research in Fluid Mechanics and Thermal Sciences* 39, no. 1 (2017): 17-25.
[18] Husaru, D. E., P. D. Bârsănescu, and D. Zahariea. "Effect of yaw angle on the global performances of Horizontal Axis Wind Turbine-QBlade simulation." In *IOP Conference Series: Materials Science and Engineering*, vol. 595, no. 1, p. 012047. IOP Publishing, 2019. https://doi.org/10.1088/1757-899X/595/1/012047
[19] Mahmuddin, Faisal. "Rotor blade performance analysis with blade element momentum theory." *Energy Procedia* 105 (2017): 1123-1129. https://doi.org/10.1016/j.egypro.2017.03.477
[20] Moriarty, Patrick J., and A. Craig Hansen. *AeroDyn theory manual*. No. NREL/TP-500-36881. National Renewable Energy Lab., Golden, CO (US), 2005. https://doi.org/10.2172/15014831
[21] Freddi, Alessandro, Mario Salmon, Alessandro Freddi, and Mario Salmon. "Introduction to the Taguchi method." *Design principles and methodologies: from conceptualization to first prototyping with examples and case studies* (2019): 159-180. https://doi.org/10.1007/978-3-319-95342-7_7
[22] Babayigit, Bilal, and Ercan Senyigit. "Design optimization of circular antenna arrays using Taguchi method." *Neural Computing and Applications* 28 (2017): 1443-1452. https://doi.org/10.1007/s00521-015-2162-y
[23] Tsai, Jinn-Tsong, Tung-Kuan Liu, and Jyh-Horng Chou. "Hybrid Taguchi-genetic algorithm for global numerical optimization." *IEEE Transactions on evolutionary computation* 8, no. 4 (2004): 365-377. https://doi.org/10.1109/TEVC.2004.826895
[24] Shamsuddin, Shahidah Arina, Mohd Nazree Derman, Uda Hashim, Muhammad Kashif, Tijjani Adam, Nur Hamidah Abdul Halim, and Muhammad Faheem Mohd Tahir. "Nitric acid treated multi-walled carbon nanotubes optimized by Taguchi method." In *AIP Conference Proceedings*, vol. 1756, no. 1, p. 090002. AIP Publishing LLC, 2016. https://doi.org/10.1063/1.4958783
[25] Khellaf, A., H. Aouici, S. Smaiah, S. Boutabba, M. A. Yallese, and M. Elbah. "Comparative assessment of two ceramic cutting tools on surface roughness in hard turning of AISI H11 steel: including 2D and 3D surface topography." *The International Journal of Advanced Manufacturing Technology* 89, no. 1-4 (2017): 333-354. https://doi.org/10.1007/s00170-016-9077-3
[26] Chandrala, Monir, Abhishek Choubey, and Bharat Gupta. "CFD analysis of horizontal axis wind turbine blade for optimum value of power." *International Journal of Energy and Environment* 4, no. 5 (2013): 825-834.
[27] Koç, Emre, Onur Günel, and Tahir Yavuz. "Comparison of Qblade and CFD results for small-scaled horizontal axis wind turbine analysis." In *2016 IEEE International Conference on Renewable Energy Research and Applications (ICRERA)*, pp. 204-209. IEEE, 2016. https://doi.org/10.1109/ICRERA.2016.7884538
[28] Takey, Mohamed, Tholudin Mat Lazim, Iskandar Shah Ishak, NAR Nik Mohd, and Norazila Othman. "Computational Investigation of a Wind Turbine Shrouded with a Circular Ring." *CFD Letters* 12, no. 10 (2020): 40-51. https://doi.org/10.37934/cfdl.12.10.4051

[29] Zakaria, Ahmad, and Mohd Shahrul Nizam Ibrahim. "Velocity Pattern Analysis of Multiple Savonius Wind Turbines Arrays." (2021). https://doi.org/10.37934/cfdl.12.3.3138

[30] Ledoux, Jeremy, Sebastián Riffo, and Julien Salomon. "Analysis of the blade element momentum theory." *SIAM Journal on Applied Mathematics* 81, no. 6 (2021): 2596-2621. https://doi.org/10.1137/20M133542X

[31] Velázquez, Miguel Toledo, Marcelino Vega Del Carmen, Juan Abugaber Francis, Luis A. Moreno Pacheco, and Guilibaldo Tolentino Eslava. "Design and experimentation of a 1 MW horizontal axis wind turbine." *Journal of Power and Energy Engineering* 2014 (2014). https://doi.org/10.4236/jpee.2014.21002

[32] Marten, David, Jan Wendler, Georgios Pechlivanoglou, Christian Navid Nayeri, and Christian Oliver Paschereit. "QBLADE: an open source tool for design and simulation of horizontal and vertical axis wind turbines." *International Journal of Emerging Technology and Advanced Engineering* 3, no. 3 (2013): 264-269.

[33] Koç, Emre, Onur Gunel, and Tahir Yavuz. "Mini-Scaled Horizontal Axis Wind Turbine Analysis By Qblade And Cfd." *International Journal of Energy Applications and Technologies* 3, no. 2 (2016): 87-92.

[34] Marten, David, Matthew Lennie, Georgios Pechlivanoglou, Christian Navid Nayeri, and Christian Oliver Paschereit. "Implementation, optimization, and validation of a nonlinear lifting line-free vortex wake module within the wind turbine simulation code qblade." *Journal of Engineering for Gas Turbines and Power* 138, no. 7 (2016). https://doi.org/10.1115/1.4031872

[35] Wendler, Juliane, David Marten, George Pechlivanoglou, Christian Navid Nayeri, and Christian Oliver Paschereit. "An unsteady aerodynamics model for lifting line free vortex wake simulations of hawt and vawt in qblade." In *Turbo Expo: Power for Land, Sea, and Air*, vol. 49873, p. V009T46A011. American Society of Mechanical Engineers, 2016. https://doi.org/10.1115/GT2016-57184

[36] Husaru, D. E., P. D. Bârsănescu, and D. Zahariea. "Effect of yaw angle on the global performances of Horizontal Axis Wind Turbine-QBlade simulation." In *IOP Conference Series: Materials Science and Engineering*, vol. 595, no. 1, p. 012047. IOP Publishing, 2019. https://doi.org/10.1088/1757-899X/595/1/012047

[37] Kaushik, Vishal, and Naren Shankar. "Statistical Analysis using Taguchi Method for Designing a Robust Wind Turbine." *Journal of Advanced Research in Fluid Mechanics and Thermal Sciences* 100, no. 3 (2022): 92-105. https://doi.org/10.37934/arfmts.100.3.92105